Chin. Geogra. Sci. 2022 Vol. 32 No. 4 pp. 592−605
https://doi.org/10.1007/s11769-022-1288-y

Springer Science Press
www.springerlink.com/content/1002-0063

A Modified Temperature-Vegetation Dryness Index (MTVDI) for Assessment of Surface Soil Moisture Based on MODIS Data

WANG Hao[1], LI Zongshan[2], ZHANG Weijuan[3], YE Xin[4], LIU Xianfeng[1]

(1. *Department of Geography*, *School of Geography and Tourism*, *Shaanxi Normal University*, *Xi'an* 710119, *China*; 2. *State Key Laboratory of Urban and Regional Ecology*, *Research Center for Eco-Environmental Science*, *Chinese Academy of Sciences*, *Beijing* 100085, *China*; 3. *College of Marxism*, *Fujian Normal University*, *Fuzhou* 350117, *China*; 4. *Nanjing Institute of Environmental Sciences*, *Ministry of Environmental Protection of the People's Republic of China*, *Nanjing* 210042, *China*)

Abstract: Spatio-temporal dynamic monitoring of soil moisture is highly important to management of agricultural and vegetation ecosystems. The temperature-vegetation dryness index based on the triangle or trapezoid method has been used widely in previous studies. However, most existing studies simply used linear regression to construct empirical models to fit the edges of the feature space. This requires extensive data from a vast study area, and may lead to subjective results. In this study, a Modified Temperature-Vegetation Dryness Index (MTVDI) was used to monitor surface soil moisture status using MODIS (Moderate-resolution Imaging Spectroradiometer) remote sensing data, in which the dry edge conditions were determined at the pixel scale based on surface energy balance. The MTVDI was validated by field measurements at 30 sites for 10 d and compared with the Temperature-Vegetation Dryness Index (TVDI). The results showed that the R^2 for MTVDI and soil moisture obviously improved (0.45 for TVDI, 0.69 for MTVDI). As for spatial changes, MTVDI can also better reflect the actual soil moisture condition than TVDI. As a result, MTVDI can be considered an effective method to monitor the spatio-temporal changes in surface soil moisture on a regional scale.

Keywords: surface soil moisture; Temperature-Vegetation Dryness Index (TVDI); vegetation index; MODIS; Modified Temperature-Vegetation Dryness Index (MTVDI)

Citation: WANG Hao, LI Zongshan, ZHANG Weijuan, YE Xin, LIU Xianfeng, 2022. A Modified Temperature-Vegetation Dryness Index (MTVDI) for Assessment of Surface Soil Moisture Based on MODIS Data. *Chinese Geographical Science*, 32(4): 592−605. https://doi.org/10.1007/s11769-022-1288-y

1 Introduction

Playing a central role in the operation of terrestrial ecosystems, soil moisture dynamic affects the soil's physical and chemical processes, and has far-reaching effect on the hydrological, climatic and environmental patterns in an area (Hassan-Esfahani et al., 2015; Feng et al., 2017; Ge et al., 2019). Due to differences in vegetation types, precipitation distribution and topography, soil moisture is highly heterogeneous on both temporal and spatial scales (Sun et al., 2014; Peng et al., 2015). Local soil moisture often determines spatial distribution and growth of vegetations over an area, this is especially the case in arid and semi-arid areas, where insufficient water supply for vegetation caused by soil water depletion may directly impair the security and health of regional ecological environments (Cao et al., 2009; Wang and Cao, 2011). Therefore, estimating and monit-

Received date: 2021-11-05; accepted date: 2022-04-09
Foundation item: Under the auspices of the National Natural Science Foundation of China (No. 41801180), the Natural Science Basic Research Plan in Shaanxi Province of China (No. 2020JQ415, 2019JQ-767)
Corresponding author: WANG Hao. E-mail: foreva@snnu.edu.cn

oring spatio-temporal distribution of regional soil moisture are highly important in management of agricultural and local ecosystems (Cho et al., 2014; Feng et al., 2016).

Most methods for monitoring soil moisture are based on field observations of sample points, but such methods are costly and time consuming. More importantly, they fail to meet the needs of studying the spatial and temporal dynamics in soil moisture at the regional scale (Merlin et al., 2010; Hsu and Chang, 2019). Therefore, the large scale determination of surface soil moisture (0–5 cm) based on microwave and optical remote sensing data has become the focus of relevant research due to advances in remote sensing technology (Han et al., 2010; Sun et al., 2014; Peng et al., 2015). However, microwave remote sensing data still have certain limitations in characterizing spatial and temporal distribution of regional surface soil moisture. For example, although active and passive microwave sensors have strong penetrating power and are affected less by weather conditions, the remote sensing data with relatively low spatial resolution (20–40 km for passive microwave sensors) and limited repeat intervals (approximately 16–25 d for active microwave sensors) may not accurate enough for many regional studies (Sun et al., 2012; Sadeghi et al., 2017). In general, low temporal and spatial resolution of the microwave data limits their application in monitoring surface soil moisture accurately.

Because of the long time span and high spatial and temporal resolution, estimating surface soil moisture based on Land Surface Temperature (T_s) and the Vegetation Index (VI) from thermal infrared and optical remote sensing data has been used widely (Son et al., 2012; Garcia et al., 2014). Previous studies have shown that T_s and VI are both important physical parameters that reflect soil moisture, and there is an obvious negative correlation between them (Price, 1990; Nemani et al., 1993). Carlson et al. (1994) and Moran et al. (1994) found that the scatter diagram with T_s and VI as the horizontal and vertical coordinates, respectively, are distributed in a triangular or trapezoidal shape. The triangular or trapezoidal space can reflect the changing trend in surface soil moisture effectively. Based on this theory, Sandholt et al. (2002) proposed the Temperature-Vegetation Dryness Index (TVDI), and estimated and monitored the dynamic changes of surface soil moisture. While thermal infrared data are susceptible to interference and the vegetation index to calculate soil moisture is hysteretic, this method, which combines optics and thermal infrared remote sensing, overcomes such shortcomings by considering the temporal-spatial resolution and time span (Li et al., 2010; Gao et al., 2011). Therefore, it applies to the soil moisture monitoring research (Petropoulos et al., 2009; Rahimzadeh-Bajgiran et al., 2012). However, fitting the dry and wet edges of the feature space is crucial to the result of TVDI. Yet most existing studies have simply used linear regression to construct empirical models to fit the edges of the feature space, requiring extensive data from a vast study area and producing subjective results. The regression result is often lower than the theoretical value, particularly when dry-edge fitting is performed, and ultimately affects the accuracy of soil moisture (Cho et al., 2014; Zhu et al., 2017a). Therefore, it is important to improve the edge fitting method of the T_s-VI feature space, and to construct a suitable dry edge fitting method in particular.

In this study, a modified index is construct, and the modification is meant to improve the performance of the TVDI. More specifically, the aims of this study are: 1) to construct a Modified Temperature-Vegetation Dryness Index (MTVDI) based on optical and thermal infrared remote sensing data to estimate surface soil moisture, and to avoid the effect of the linear regression method in dry edge fitting; 2) to evaluate the effectiveness of MTVDI after a comparison of MTVDI and TVDI index results based on soil moisture data measured at the sample sites. The results of this study will provide a reference for regional surface soil moisture remote sensing simulation studies.

2 Study Area and Data

2.1 Study area

The study area is located in the Yan'an section of the Yanhe River Basin (109°10′E to 109°55′E, 36°20′N to 37°10′N) of China (Fig. 1). The climate type of the study area belongs to a typical warm temperate continental monsoon climate, with an average annual precipitation 500 mm decreasing gradually from southwest to northeast. The annual average temperature in the region is 7.7°C to 10.6°C. The primary vegetation types in this

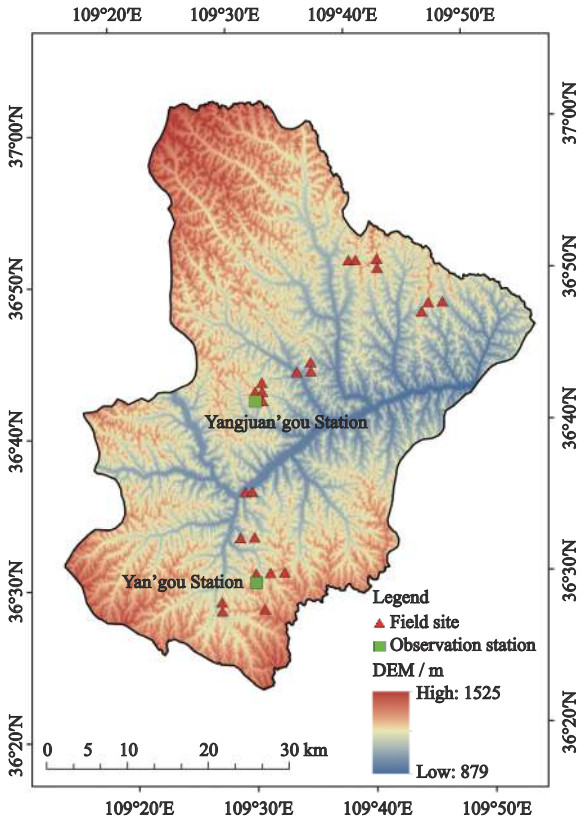

Fig. 1 Location of the study area and the field measurement sites

area include deciduous broad-leave forest, coniferous forest, and shrub grassland. The principal soil type is loessal soil, which has a uniform texture but poor fertility (Wang and Ren, 2006).

2.2 Data sources

2.2.1 Field measurement data

The study area is in the Yan'an section of the Yanhe River Basin. Surrounding two major observation stations in the Yangjuangou and Yangou catchment area, 30 measurement sites were set covering the study area (Fig. 1). When setting sample sites, based on a comprehensive survey of the sites, sample sites were evenly arranged in different geomorphic units, covering different vegetation types including grassland, shrub and woodland. The locations and vegetation types of all measurement sites are shown in Table 1. Two automatic weather stations and several soil moisture sensors were installed at the measurement sites in the Yangjuangou station. The soil moisture was measured continuously at six different depths in the soil profile: 5, 20, 40, 60, 80, and 100 cm. At other measurement points, the soil moisture was measured with a TDR 300 soil moisture meter every 15 d during the plant growing season in 2015 (May to September). Only the surface soil moisture data (0–5 cm), which were measured at the time closest to the satellite overpass time, were used in this study. Considering that the resolution of remote sensing data is 1 km, these sample points were designed with a range of about 200 × 200 m when collecting data in the field. Soil moisture samples were taken every 50 m on the diagonal, and 8–10 samples were collected in each sample site. The abnormal values were eliminated and the remaining values were averaged to obtain the soil moisture of

Table 1 Locations and vegetation types of measurement sites

Sites	Vegetation type	Longitude / °E	Latitude / °N
Yangjuangou	Grass	109.52	36.70
	Shrub	109.53	36.70
	Grass	109.52	36.71
	Grass	109.52	36.71
	Forest	109.52	36.71
	Forest	109.52	36.71
	Grass	109.52	36.71
	Grass	109.53	36.71
	Forest	109.53	36.72
	Shrub	109.50	36.60
	Grass	109.51	36.60
	Grass	109.58	36.73
	Forest	109.60	36.73
	Forest	109.60	36.74
Yangou	Forest	109.52	36.47
	Shrub	109.52	36.47
	Forest	109.51	36.51
	Forest	109.53	36.51
	Shrub	109.55	36.51
	Forest	109.51	36.55
	Forest	109.49	36.55
	Shrub	109.46	36.47
	Forest	109.46	36.48
Huangjiagou	Forest	109.79	36.80
	Shrub	109.76	36.79
	Grass	109.77	36.80
Changgou	Forest	109.70	36.85
	Grass	109.70	36.84
	Forest	109.66	36.85
	Forest	109.67	36.85

the sample site. In this way, the soil moisture in the pixel is reflected to the utmost extent in accuracy.

2.2.2 Remote sensing data

The parameters involved in this study were all constant or can be obtained based on MODIS remote sensing data, except for wind speed data as derived from meteorological data obtained from the China Meteorological Data Sharing Network (http://data.cma.cn/) and field measurements. The MODIS data can be downloaded from NASA Earth Science Data (https://earthdata.nasa.gov/) and the Resource and Environment Science and Data Center (http://www.resdc.cn/Default.aspx). The six MODIS products, including daily geolocation at 1 km resolution (MOD03), daily cloud at 1 km resolution (MOD06), daily temperature and water vapor profile at 5 km resolution (MOD07), daily land surface temperature at 1 km resolution (MOD11), 8-d albedo at 1 km resolution (MOD43), and 16-d vegetation indices (NDVI) at 1 km resolution (MOD13), were used to estimate the solar zenith angle, land surface temperature, atmospheric temperature, dew point temperature, surface albedo, and vegetation coverage, respectively (Table 2) (Zhu et al., 2017a). The spatial resolution of all remote data was set to 1 km. To ensure the accuracy of the result, 10 d during the plant growing season (May to September) in 2015 that coincided with the field measurement date when cloud cover was less than 20% were selected: DOY (Day of Year) 124, 144, 155, 169, 188, 206, 217, 227, 255, and 269 (Sun et al., 2012). Other parameters involved in this study all can be regarded as constants based on previous studies (Prince et al., 1998; Zhang et al., 2008; Sun et al., 2012).

3 Theoretical Background

3.1 Theory of TVDI

Following the concept of traditional TVDI, Long and Singh (2012) proposed a conceptual sketch of the trapezoid $T_s - f_c$ space in their study, and the concept is shown in Fig. 2. For an area, the left and right edges (AC and BD) of the trapezoidal feature space represent the changes in T_s on the bare soil and fully covered surface, respectively. Generally, as the Fractional Vegetation Cover (f_c) increases, the vegetation canopy's absorption of solar energy leads to a higher canopy temperature. Meanwhile, such increase of temperature can be offseted by vegetation transpiration. Therefore, when soil moisture is insufficient, evapotranspiration weakens and vegetation canopy temperature increases; otherwise, evapotranspiration strengthens and canopy temperature decreases. Upper edge (AB, dry edge) represents upper limit of surface temperature that can be reached at a given coverage. Lower edge (CD) represents lower limit of surface temperature that can be reached under the condition of unlimited maximum soil moisture, which is the wet edge that usually assumed to be equal due to the saturated wet condition (Zhu et al., 2017c). The soil moisture trapezoidal space of each f_c pixel is formed. In the trapezoidal space, $T_{s\max}$ and $T_{s\min}$ are the bare soil surface temperature under the driest and wettest conditions respectively. $T_{c\max}$ and $T_{c\min}$ are the fully covered surface temperature under the driest and wettest conditions. The f_c and T_s values of each pixel in the area will be distributed in the $T_s - f_c$ feature space

Table 2 Data statistics for estimating MTVDI

Variable	Datasets	Preparation	Sources
Fractional Vegetation Cover (f_c)	MODIS data 16-day vegetation indices (NDVI) at 1 km resolution (MOD13)	Calculated referring Shifaw et al. (2018)	Resource and Environment Science and Data Center (http://www.resdc.cn/Default.aspx)
Albedo of the bare land surface (α_s)	MODIS data 8-day albedo at 1 km resolution (MOD43)	Directly derived from MOD43	NASA Earth Science Data (https://earthdata.nasa.gov/)
Air temperature (T_a)	MODIS data daily cloud at 1 km resolution (MOD06), daily temperature and water vapor profile at 5 km resolution (MOD07)	Calculated referring Zhu et al. (2017b) based on MOD06 and MOD07	NASA Earth Science Data (https://earthdata.nasa.gov/)
Solar zenith angle (θ)	MODIS data daily geolocation at 1 km resolution (MOD03)	Directly derived from MOD03	NASA Earth Science Data (https://earthdata.nasa.gov/)
Dew point temperature (T_d)	MODIS data daily temperature and water vapor profile at 5 km resolution (MOD07)	Directly derived from MOD07	NASA Earth Science Data (https://earthdata.nasa.gov/)

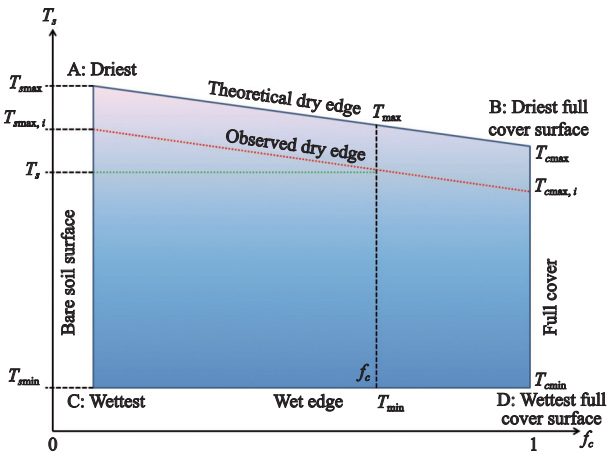

Fig. 2 An illustration of the trapezoid $T_s - f_c$ feature space. Upper edge (AB) and lower edge (CD) represent the dry and wet edges of the $T_s - f_c$ feature space, respectively. T_{smax} and T_{smin} are the bare soil surface temperature under the driest and wettest conditions. T_{cmax} and T_{cmin} are the fully covered surface temperature under the driest and wettest conditions

composed of four poles of A, B, C, and D, and isopleths of soil moisture can be retrieved by the TVDI (Sandholt et al., 2002). The calculation formula is as follows:

$$TVDI = \frac{T_s - T_{\min}}{T_{\max} - T_{\min}} \tag{1}$$

$$T_{\max} = a + b \times f_c \tag{2}$$

$$f_c = \frac{NDVI - NDVI_{\min}}{NDVI_{\max} - NDVI_{\min}} \tag{3}$$

where T_s is the surface temperature of a given pixel, and $T_{\min}$ is the minimum surface temperature along the wet side, where $T_{\min} = T_{smin} = T_{cmin} = T_w$ (wet edge temperature). $T_{\max}$ is the maximum surface temperature. a and b are parameters defining the dry edge modelled as a linear fit to data. TVDI ranges from 0 to 1. $NDVI_{\min}$ is the minimum NDVI value for bare soil, and $NDVI_{\max}$ is the maximum NDVI value for a fully vegetated surface.

3.2 The development of MTVDI

Following Fig. 2, the observed dry edge of the $T_s - f_c$ feature space indicates an extreme water stressed condition, in which vegetation has no evapotranspiration cooling effect and the T_s reaches its max value. However, vegetation exhibits zero evapotranspiration rarely in actual conditions (Stisen et al., 2008). Therefore, the observed dry edge value calculated based on Eq. (2) is likely to be lower than the theoretical dry edge value. To improve the accuracy of the calculation results, the dry edge can be determined with Eq. (4) (Zhang et al., 2008; Long and Singh, 2012; Sun et al., 2012; Zhu et al., 2017a).

$$T_{\max} = T_{s\max} + f_c(T_{c\max} - T_{s\max}) \tag{4}$$

In this equation, $T_{\max}$ was divided into two parts, the driest full vegetation cover surface temperature (T_{cmax}) and the driest bare soil surface temperature (T_{smax}), which indicates that in the case of relatively uniform soil moisture and meteorological conditions, the change of the T_s in the area is mainly affected by the f_c. Thus, the T_s value under the same soil moisture condition can be expressed as the sum of T_{cmax} and T_{smax} weighted by vegetation coverage (Moran et al., 1994; Anderson et al., 2007).

Based on the theories above, we used the MTVDI method to estimate surface soil moisture. Previous studies have shown that under uniform soil moisture and atmospheric conditions, due to the difference in thermal conductivity between soil and canopy, the surface temperature of pixels within the same soil moisture contour is mainly controlled by vegetation coverage. The remote sensed T_s tends to approach the air temperature as the vegetation cover increases, and the radiation temperature of a full vegetated canopy is in equilibrium with the temperature of the air within the canopy (Czajkowski et al., 1997; Prihodko and Goward, 1997; Prince et al., 1998). Therefore, T_{cmax} in Equation 4 can be replaced by the air temperature (T_a) for a given pixel and Eq. (4) can be converted to:

$$T_{\max} = f_c T_a + (1 - f_c) T_{s\max} \tag{5}$$

Combine Eq. (5) with Eq. (1):

$$MTVDI = \frac{T_s - T_{\min}}{(f_c T_a + (1 - f_c) T_{s\max}) - T_{\min}} \tag{6}$$

In the original TVDI, the $T_{\max}$ of dry edge is mostly estimated by the regression method as shown in Eq. (2). A sufficient amount of data is needed for regression analysis to determine the $T_{\max}$ regression equation. In this study, MTVDI was adopted to determine the method to estimate the dry edge ($T_{\max}$) from the pixel scale. This reduced the dependence on data volume, and more objective than is the regression method, which is helpful to improve the estimation accuracy of surface soil moisture. Based on Zhu et al. (2017b), a simple parameterization scheme of T_a was developed based entirely on MODIS data (MOD06 and MOD07) without

ancillary data. Therefore, in Eq. (6), T_s and T_a can be obtained or estimated from MODIS data, and f_c can be calculated from MODIS NDVI data. Only the parameters of the driest bare soil surface temperature (T_{smax}) and T_{min} need to be obtained further in MTVDI. The derivation process of MTVDI is showed in Fig. 3.

3.3 Calculation of T_{smax} and T_{min}

Based on the surface energy balance principle, T_s can be estimated according to the following formula (Long and Singh 2012):

$$T_s = \frac{(1-\alpha)S_d + \varepsilon_s\varepsilon_a\sigma T_a^4 - \varepsilon_s\sigma T_a^4 - LE/(1-c)}{4\varepsilon_s\sigma T_a^3 + \rho c_p/(r_a(1-c))} + T_a \quad (7)$$

where α is the land surface albedo, which is unitless; S_d indicates the downward shortwave radiation (W/m^2); ε_s and ε_a are the land surface and atmosphere emissivity, which are both unitless; σ represents the Boltzmann constant, which is 5.67 × 10^{-8} W/(m^2·K^4) (Zhu et al., 2017a); T_a is the air temperature (K); LE is the latent heat flux (W/m^2); c is conversion ratio; ρ indicates the air density (kg/m^3); c_p represents the heat capacity of constant pressure air (J/(kg·K)), and r_a is the aerodynamic drag (s/m).

Because T_{smax} represents the maximum surface temperature under extremely dry conditions for bare soil, the parameters in Eq. (7) can be replaced with parameters under dry and bare soil conditions. Therefore, the energy consumed by LE can be assumed to be 0, and Eq. (7) can be converted to:

$$T_{smax} = \frac{(1-\alpha_s)S_d + \varepsilon_{ss}\varepsilon_a\sigma T_{amax}^4 - \varepsilon_{ss}\sigma T_{amax}^4}{4\varepsilon_{ss}\sigma T_{amax}^3 + \rho c_p/(r_{as}(1-c_s))} + T_{amax} \quad (8)$$

in which ε_{ss} and c_s are limited by the properties of bare and dry soil, which are 0.95 and 0.315, respectively (Zhang et al., 2008; Sun et al., 2012). α_s and r_{as} are the albedo and aerodynamic drag of the bare land surface. In this study, α_s was extracted from MODIS data, while r_{as} was estimated as follows (Brutsaert, 1982):

$$r_{as} = \frac{(\ln((z-d)/z_{0m}) - \varphi_m)^2}{k^2 u} \quad (9)$$

in which z (m) is the reference height; d (m) is the zero-plane displacement height, which is 0 for bare soil; z_{0m} (m) is the surface roughness length of momentum, which is 0.005 for bare soil; k is the von Karman constant (0.41); u (m / s) is the wind speed at the reference height, which is obtained from meteorological data, and

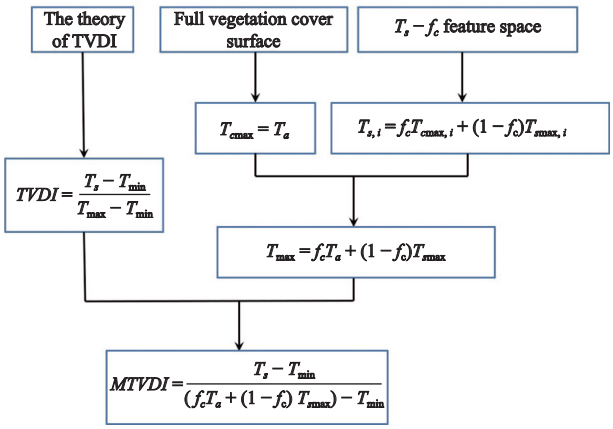

Fig. 3 The derivation process of MTVDI (Modified Temperature-Vegetation Dryness Index). T_{cmax} and T_{smax} are the fully covered and bare soil surface temperature under the driest condition

φ_m is the stability correction function.

The equations to calculate S_d and ε_a are:

$$S_d = \frac{S_0 cos^2\theta}{1.085cos\theta + e_0(2.7 + cos\theta) \times 10^{-3} + \beta} \quad (10)$$

$$e_0 = 6.11\exp\left(\frac{L_v}{R_v}\left(\frac{1}{273.15} - \frac{1}{T_d}\right)\right) \quad (11)$$

$$\delta = \frac{46.5}{T_a} e_0 \quad (12)$$

$$\varepsilon_a = 1 - (1+\delta)exp(-\sqrt{(1.2+3\delta)}) \quad (13)$$

in which S_0 is the solar radiation constant at the top of the atmosphere, which is 1367 (W/m^2). θ is the solar zenith angle. β (0.1) is the dimensionless constant. δ and e_0 is the saturation vapor pressure (hPa/K) and near surface vapor pressure (hPa), respectively. L_v and R_v is the latent heat of vaporization and the gas constant of water vapor, which are 2.5 × 10^6 (J/kg) and 461 (J/kg·K), respectively. T_d is the dew point temperature.

T_{min} can also be calculated based on the energy balance principle, but the relevant calculation parameters are difficult to obtain. However, following Fig. 2, it can be assumed that $T_{min} = T_{smin} = T_{cmin} = T_w$ (wet edge temperature). Previous research has shown that for a certain area, the greater the surface evapotranspiration rate, the smaller the difference between surface and atmospheric temperature (Zhang et al., 2008; Long and Singh 2012; Sun et al., 2012). As T_{min} represents the surface temperature at maximum humidity, a water body can be considered an ideal surface with such characteristics. Therefore, the average temperature of permanent open

water extracted from the land use data can be regarded as the wet edge in the study area ($T_{min} = T_{smin} = T_{cmin} = T_w$).

4 Results

4.1 Analysis of the feature space

The $T_s - f_c$ feature space of the 10 days selected was established in this study. Based on the theories of Zhang et al. (2008) and Long and Singh (2013), the theoretical limiting edges determined by the energy balance principle were calculated. The observed dry edges of the scatter plot feature space were determined with the method proposed in previous studies (Sandholt et al., 2002; Tang et al., 2010). The determination of the wet edge is easier compared to that of the dry edge. As exposited in section 2.2, $T_{min} = T_{smin} = T_{cmin} = T_w$, and the temperature of the theoretical and observed wet edge is equal, which can be considered as the surface temperature of the water body. Therefore, the mean temperature of the permanent open water extracted from the land use data was adopted as the wet edge in the study area.

For comparison purpose, the variation of the intercept of the theoretical dry edge and the observed dry edges determined from TVDI and MTVDI are presented in Fig. 4. In general, the intercepts of the theoretical dry edge and the two observed dry edges have similar variation trend. Yet it is worth noting that the variation trend of the intercept determined from MTVDI is more consistent with the theoretical dry edge. The correlation coefficient between these two intercepts is 0.98, and the RMSE (Root Mean Square Error) is 5.22 K, while the correlation coefficient and *RMSE* between the observed dry edge intercept determined from TVDI and the theoretical dry edge is 0.94 K and 7.29 K, respectively. Therefore, the relationship between the observed dry edge intercept determined from MTVDI and the theoretical dry edge is much closer.

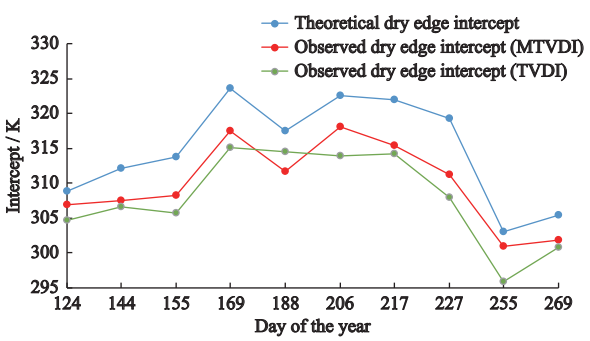

Fig. 4 Comparison of the intercept determined by three different dry edges

The results of the MTVDI feature space showed that the theoretical dry edges and wet edges can form a clear trapezoidal space on all 10 d (Fig. 5). However, as the observed dry edges depend on the distribution of scatter plots, they do not form a regular trapezoid on all days. For example, the feature space shape tended to be more rectangular on DOY 169 and 188. The distribution pattern of the scatter plots also showed that by reason of the relatively high vegetation coverage in the study area, and because it was the growing season with higher temperatures during the study period, most of the points were concentrated in areas with a vegetation coverage higher than 50%, and the T_s value was relatively high (approximately 300 K). Meanwhile, at the end of the growing season (DOY 255 and 269), the T_s value was relatively low (most points < 300 K), and the points had a narrow distribution.

4.2 Comparison with field measurement data

Because of the differences in spatial scale and physical amount between field measurement data and remote sensing data, correlation analysis is used to verify the accuracy of remote sensing retrieved soil water stress index (Rahimzadeh-Bajgiran et al., 2013; Zhu et al., 2017c). Fig. 6 presents the scatter plot of TVDI, MTVDI, and soil moisture measured over all sites. In general, the results of MTVDI and TVDI were consistent, and both were correlated negatively with soil moisture. Yet still the MTVDI produced better results, with more concentrated scatterplots than the TVDI, and the coefficient of determination (R^2) for MTVDI and soil moisture (0.69) was higher than that for TVDI (0.45). The range in the values of TVDI, MTVDI, field-measured soil moisture, and the R^2 between these two indices and soil moisture for all 10 d are shown in Table 3. With the value of R^2, both TVDI and MTVDI reflected the spatial change in soil moisture on most days, except for DOY 124, when the R^2 obtained from both TVDI and MTVDI were small (0.21 and 0.22, respectively). In addition, except for DOY 144, the R^2 between MTVDI and soil moisture was apparently higher than that achieved by TVDI on other days. Especially on DOY 155, 169, and 255, the difference in R^2 obtained by these two indices was greater than 0.2, which indicates that MTVDI can reflect the spatial

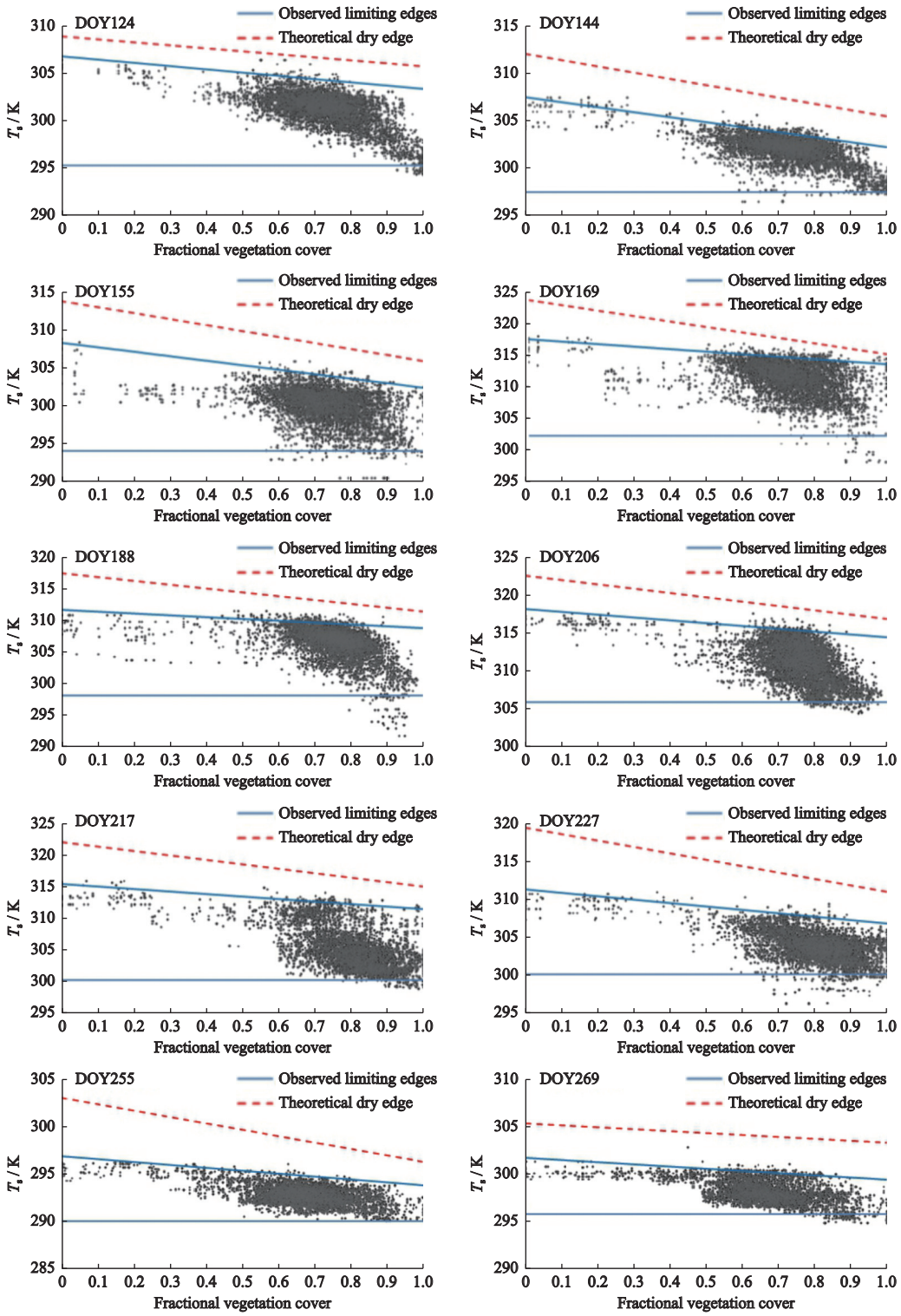

Fig. 5 The $T_s - f_c$ feature space of the 10 selected DOY (day of year). T_s is the land surface temperature, and f_c is the fractional vegetation cover

change in soil moisture more effectively than TVDI.

4.3 Spatial comparison between TVDI and MTVDI

To further compare the difference in spatial distribution between TVDI and MTVDI, the average TVDI and MTVDI of all 10 d in this study are presented in Fig. 7. The TVDI ranged from 0.19 to 0.96, while the MTVDI ranged from 0.56 to 0.95. The mean value of MTVDI

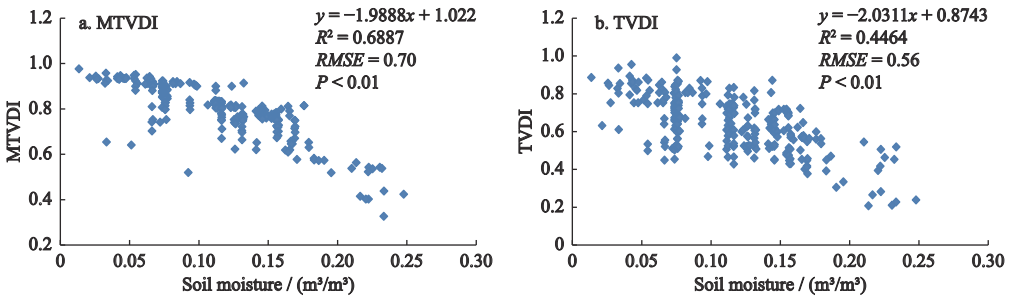

Fig. 6 Relationship between MTVDI and TVDI (Temperature-Vegetation Dryness Index) to soil moisture

Table 3 Value range of TVDI, MTVDI, and field measurement soil moisture, and R^2 between TVDI, MTVDI, and soil moisture

DOY	TVDI		MTVDI		Soil moisture value range
	R^2	Value range	R^2	Value range	
124	0.21	0.43–0.81	0.22	0.70–0.90	0.07–0.18
144	0.50	0.61–0.99	0.37	0.66–0.86	0.08–0.16
155	0.40	0.32–0.88	0.68	0.62–0.95	0.08–0.18
169	0.36	0.62–0.96	0.58	0.75–0.96	0.03–0.16
188	0.52	0.57–0.89	0.67	0.79–0.98	0.02–0.15
206	0.56	0.16–0.82	0.66	0.42–0.95	0.07–0.25
217	0.47	0.15–0.69	0.62	0.33–0.92	0.05–0.23
227	0.49	0.50–0.83	0.58	0.75–0.94	0.02–0.15
255	0.36	0.25–0.88	0.65	0.40–0.91	0.05–0.22
269	0.52	0.40–0.75	0.66	0.54–0.88	0.07–0.23

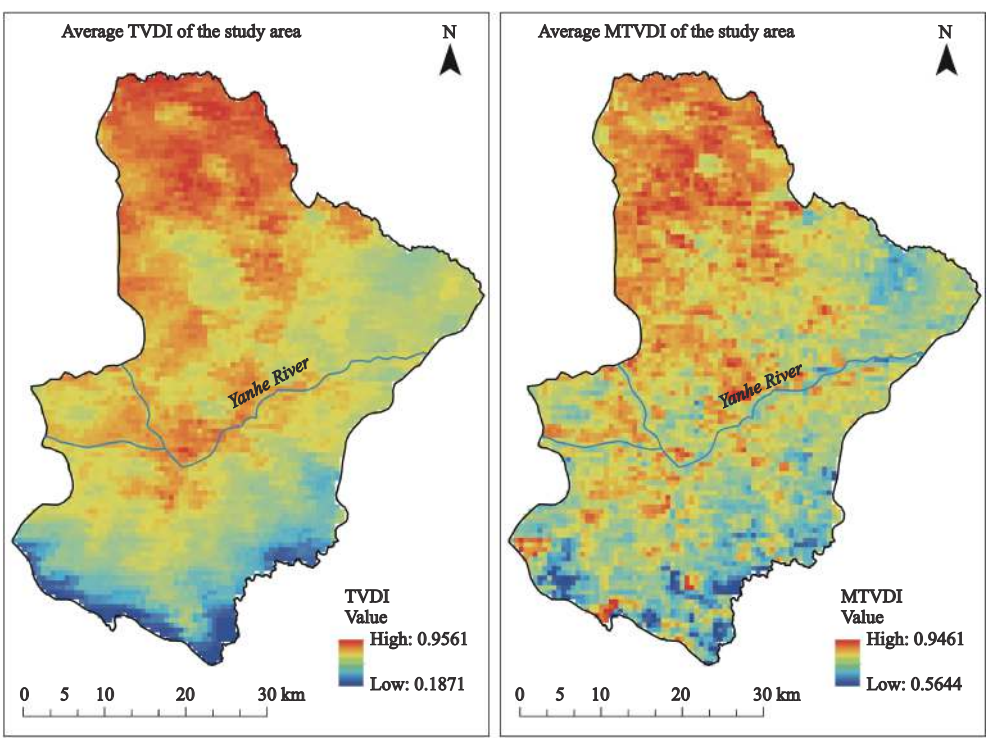

Fig. 7 Spatial distribution of average TVDI and MTVDI on 10 selected DOY

was much higher than that of TVDI, which is 0.81 and 0.66 respectively. The distributions of TVDI and MTVDI had similar spatial patterns. Both high values of these two indices were distributed primarily in the north, indicating that the southern part of the study area has higher soil moisture. However, the spatial distribution of MTVDI showed that there is a linear low-value area in the middle of the study area, indicating a feature that the soil is moister than the surrounding area. This feature, consistent with the location of the Yanhe River in the study area, and can not be found in the spatial distribution of TVDI. It therefore leads to the conclusion that the MTVDI distribution better reflects the actual soil moisture condition.

5 Discussion

According to the description of $T_s - f_c$ feature space, it can be concluded that both TVDI and MTVDI only represent the water stress index of relative soil moisture. It should be noted that TVDI and MTVDI is not the same as the volumetric soil moisture measured in the field (Mallick et al., 2009). They have a significant negative correlation with soil moisture. The higher the TVDI and MTVDI values are, the lower the relative soil moisture is. Three land cover types are involved in this study (forest, grassland, and shrub). To analyze the performance of MTVDI, scatter plots of average MTVDI, TVDI and soil moisture of different land cover types in 10 selected days were calculated (Fig. 8). The results showed that, soil moisture is relatively low for all land cover types, which is consistent with the results of previous studies. Due to the increase of soil water consumption caused by climate change and large-scale vegetation restoration, soil moisture of almost all land cover types in the Loess Plateau is at a low level, and therefore there is no significant difference in soil moisture among different land cover types (Yu et al., 2020; Qiu et al., 2021; Zhang et al., 2020). Meanwhile, the value of MTVDI is generally higher than that of TVDI, though both values show a good consistency with the variation of soil moisture, the variation trend of MTVDI is more similar to that of soil moisture. Overall, though MTVDI does not produce significant differences among varied land cover types due to the characteristics of the Loess Plateau region, MTVDI's sensitivity to soil moisture changes is better than that of TVDI.

Although the values produced by MTVDI and TVDI are different from the measured soil moisture, due to their good indication of soil moisture, this type of index has been widely used in environmental monitoring research related to drought and soil moisture (Amani et al., 2017; Chen et al., 2011; Gao et al., 2011; Wang et al., 2016). In this study, compared with TVDI, the coef-

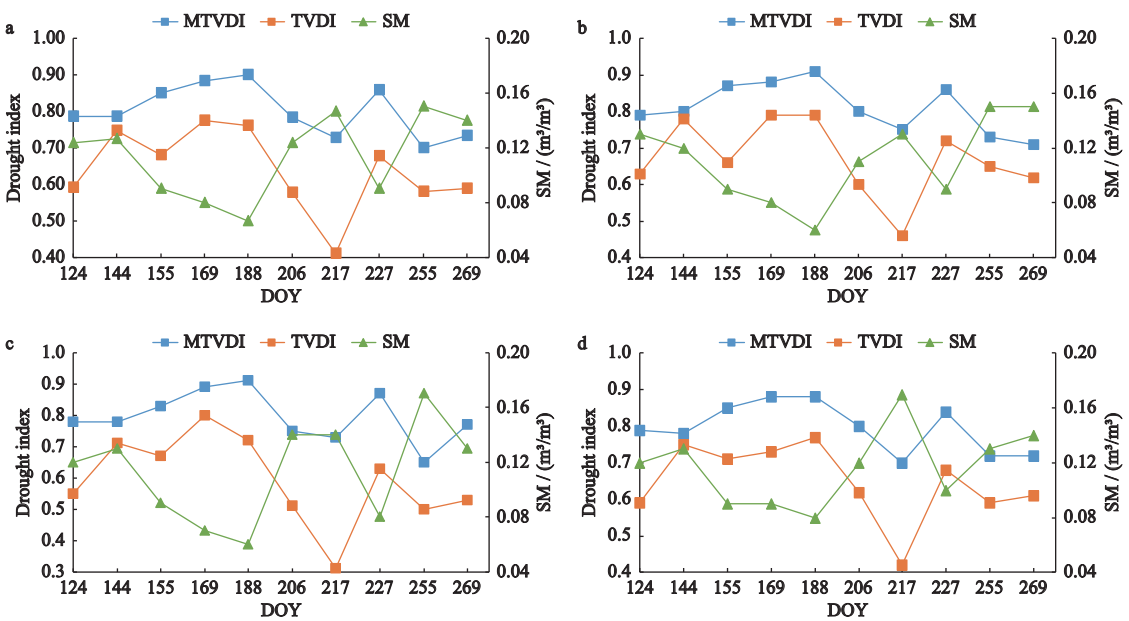

Fig. 8 Scatterplots established between average MTVDI, TVDI and soil moisture (SM) in different land cover types: (a) all land cover types, (b) Forest, (c) Grassland, and (d) Shrubs

ficient of determination (R^2) of MTVDI and soil moisture relatively improved (Fig. 7). However, in some cases, the R^2 between MTVDI and soil moisture remained low, such as DOY 124 and 144 in Table 2. Several factors are related to the errors, including the scale mismatch, accuracy of the remote sensing data, and limitation of the dry edge determination.

In general, the field measurement data can represent only a limited space of several square meters around the measurement site. In this study, each sampling site was measured repeatedly at least 3 times in the range of 200 m × 200 m to obtain the mean value of soil moisture. However, compared with the remote sensing data with a resolution of 1km, errors are still introduced when site data are used to validate the estimated results.

Uncertainties in the remote sensing data may introduce errors as well. The parameters include T_s and f_c in this study were all calculated from MODIS data. However, the actual topography of the study area is relatively complex. Factors such as changes in vegetation types and topography will cause errors between remote sensing data and actual conditions, and affect the calculation results of the parameters used in the study. Meanwhile, the estimation method will also affect the accuracy of the results besides the quality of MODIS data. For example, in this study, f_c was calculated based on Eq. (3). The maximum and minimum values of NDVI should be determined in the calculation. However, the maximum and minimum values in NDVI images cannot be directly selected as $NDVI_{max}$ and $NDVI_{min}$ (Jiang et al., 2017). It is generally considered that the NDVI value of bare land and all vegetation covered area are the minimum and maximum values respectively (Ren et al., 2021). A NDVI frequency histogram will make more accurate statistics on the corresponding NDVI values of non-vegetation coverage and full vegetation coverage areas in remote sensing images. Based on previous research experience, NDVI values corresponding to 1% and 99% of the cumulative frequency values were took as $NDVI_{min}$ and $NDVI_{max}$ in this study (Jiang et al., 2017; Shifaw et al., 2018). Obviously, different NDVI cumulative frequency values will affect the calculation results of f_c (e.g., 0.5% and 99.5% of the cumulative frequency values were took as $NDVI_{min}$ and $NDVI_{max}$), and then affect the accuracy of MTVDI. In future study, more validation should be performed about the effect of f_c estimation results on the accuracy of MTVDI.

In addition, monitoring surface soil moisture based on the $T_s - f_c$ feature space assumes an ideal environment, in which the meteorological parameters and land surface characteristics are homogeneous (Friedl and Davis, 1994; Lambin and Ehrlich, 1995). This assumption simplifies the relation between soil moisture and land surface temperature. However, the actual land surface characteristics of the study area are more complex, and the difference between theory and actual characteristics will inevitably cause some uncertainty in the determination of dry edges. In order to improve the accuracy of the MTVDI, more theoretical and test work should be done in the future.

6 Conclusions

To improve the performance of surface-temperature-vegetation index in detecting the surface soil moisture, this study constructed a Modified Temperature-Vegetation Dryness Index by using the MODIS series data. Concentrating on the $T_s - f_c$ feature space, the study adopted a more objective method to estimate the dry edge aiming to reduce the dependence on data volume and improve the accuracy of the estimation of surface soil moisture. The MTVDI was validated with the field measurement data and compared with TVDI. The results showed that the theoretical dry edges and wet edges could form a clear trapezoidal space. Meanwhile, the coefficient of determination (R^2) achieved by the MTVDI (0.69) is generally higher than that achieved by the TVDI (0.45). With respect to spatial distribution, the MTVDI also reflects the soil moisture condition better than TVDI. Therefore, MTVDI can be considered as an effective method to carry out continuous monitoring of surface soil moisture in a large area. There are still some limitations to the use of MTVDI, such as the accuracy of the remote sensing data, and the limitation of the dry edge determination. To improve the accuracy of the MTVDI, more theoretical and experimental work need to be conducted in the future.

References

Amani M, Salehi B, Mahdavi S et al., 2017. Temperature-vegetation-soil Moisture Dryness Index (TVMDI). *Remote Sensing of Environment*, 197: 1–14. doi: 10.1016/j.rse.2017.05.026

Anderson M C, Norman J M, Mecikalski J R et al., 2007. A climatological study of evapotranspiration and moisture stress across the continental United States based on thermal remote sensing: 1. Model formulation. *Journal of Geophysical Research:Atmospheres*, 112(D10): D10117. doi: 10.1029/2006JD007506

Brutsaert W, 1982. *Evaporation into the Atmosphere: Theory, History and Applications*. Netherlands: Springer. doi: 10.1007/978-94-017-1497-6

Cao S X, Chen L, Yu X X, 2009. Impact of China's Grain for Green Project on the landscape of vulnerable arid and semi-arid agricultural regions: a case study in northern Shaanxi Province. *Journal of Applied Ecology*, 46(3): 536–543. doi: 10.1111/j.1365-2664.2008.01605.x

Carlson T N, Gillies R R, Perry E M, 1994. A method to make use of thermal infrared temperature and NDVI measurements to infer surface soil water content and fractional vegetation cover. *Remote Sensing Reviews*, 9(1−2): 161–173. doi: 10.1080/02757259409532220

Chen J, Wang C Z, Jiang H et al., 2011. Estimating soil moisture using Temperature-Vegetation Dryness Index (TVDI) in the Huang-Huai-Hai (HHH) plain. *International Journal of Remote Sensing*, 32(4): 1165–1177. doi: 10.1080/01431160903527421

Cho J, Lee Y W, Lee H S, 2014. Assessment of the relationship between thermal-infrared-based temperature-vegetation dryness index and microwave satellite-derived soil moisture. *Remote Sensing Letters*, 5(7): 627–636. doi: 10.1080/2150704X.2014.950760

Czajkowski K P, Mulhern T, Goward S N et al., 1997. Validation of the Geocoding and Compositing System (GEOCOMP) using contextual analysis for AVHRR images. *International Journal of Remote Sensing*, 18(14): 3055–3068. doi: 10.1080/014311697217206

Feng X M, Fu B J, Piao S L et al., 2016. Revegetation in China's Loess Plateau is approaching sustainable water resource limits. *Nature Climate Change*, 6(11): 1019–1022. doi: 10.1038/nclimate3092

Feng X M, Li J X, Cheng W et al., 2017. Evaluation of AMSR-E retrieval by detecting soil moisture decrease following massive dryland re-vegetation in the Loess Plateau, China. *Remote Sensing of Environment*, 196: 253–264. doi: 10.1016/j.rse.2017.05.012

Friedl M A, Davis F W, 1994. Sources of variation in radiometric surface temperature over a tallgrass prairie. *Remote Sensing of Environment*, 48(1): 1–17. doi: 10.1016/0034-4257(94)90109-0

Gao Z Q, Gao W, Chang N B, 2011. Integrating temperature vegetation dryness index (TVDI) and regional water stress index (RWSI) for drought assessment with the aid of LANDSAT TM/ETM+ images. *International Journal of Applied Earth Observation and Geoinformation*, 13(3): 495–503. doi: 10.1016/j.jag.2010.10.005

Garcia M, Fernández N, Villagarcía L et al., 2014. Accuracy of the Temperature-Vegetation Dryness Index using MODIS under water-limited vs. energy-limited evapotranspiration conditions. *Remote Sensing of Environment*, 149: 100–117. doi: 10.1016/j.rse.2014.04.002

Ge X Y, Wang J Z, Ding J L et al., 2019. Combining UAV-based hyperspectral imagery and machine learning algorithms for soil moisture content monitoring. *PeerJ*, 7: e6926. doi: 10.7717/peerj.6926

Han Y, Wand Y Q, Zhao Y S, 2010. Estimating Soil Moisture Conditions of the Greater Changbai Mountains by Land Surface Temperature and NDVI. *IEEE Transactions on Geoscience & Remote Sensing*, 48(6): 2509–2515. doi: 10.1109/TGRS.2010.2040830

Hassan-Esfahani L, Torres-Rua A, Jensen A et al., 2015. Assessment of surface soil moisture using high-resolution multi-spectral imagery and artificial neural networks. *Remote Sensing*, 7(3): 2627–2646. doi: 10.3390/rs70302627

Hsu W L, Chang K T, 2019. Cross-estimation of soil moisture using thermal infrared images with different resolutions. *Sensors and Materials*, 31(2): 387–398. doi: 10.18494/SAM.2019.2090

Jiang M C, Tian S F, Zheng Z J et al., 2017. Human activity influences on vegetation cover changes in Beijing, China, from 2000 to 2015. *Remote Sensing*, 9(3): 271. doi: 10.3390/rs9030271

Lambin E F, Ehrlich D, 1995. Combining vegetation indices and surface temperature for land-cover mapping at broad spatial scales. *International Journal of Remote Sensing*, 16(3): 573–579. doi: 10.1080/01431169508954423

Li H J, Li C Q, Lin Y et al., 2010. Surface temperature correction in TVDI to evaluate soil moisture over a large area. *Journal of Food, Agriculture & Environment*, 8(3−4): 1141–1145.

Long D, Singh V P, 2012. A two-source trapezoid model for evapotranspiration (TTME) from satellite imagery. *Remote Sensing of Environment*, 121: 370–388. doi: 10.1016/j.rse.2012.02.015

Long D, Singh V P, 2013. Assessing the impact of end-member selection on the accuracy of satellite-based spatial variability models for actual evapotranspiration estimation. *Water Resources Research*, 49(5): 2601–2618. doi: 10.1002/wrcr.20208

Mallick K, Bhattacharya B K, Patel N K, 2009. Estimating volumetric surface moisture content for cropped soils using a soil wetness index based on surface temperature and NDVI. *Agricultural & Forest Meteorology*, 149(8): 1327–1342. doi: 10.1016/j.agrformet.2009.03.004

Merlin O, Al Bitar A, Walker J P et al., 2010. An improved algorithm for disaggregating microwave-derived soil moisture

based on red, near-infrared and thermal-infrared data. *Remote Sensing of Environment*, 114(10): 2305–2316. doi: 10.1016/j.rse.2010.05.007

Moran M S, Clarke T R, Inoue Y et al., 1994. Estimating crop water deficit using the relation between surface-air temperature and spectral vegetation index. *Remote Sensing of Environment*, 49(3): 246–263. doi: 10.1016/0034-4257(94)90020-5

Nemani R, Pierce L, Running S et al., 1993. Developing satellite-derived estimates of surface moisture status. *Journal of Applied Meteorology and Climatology*, 32(3): 548–557. doi: 10.1175/1520-0450(1993)032<0548:DSDEOS>2.0.CO;2

Peng J, Niesel J, Loew A et al., 2015. Evaluation of satellite and reanalysis soilmoisture products over southwest China using ground-basedmeasurements. *Remote Sensing*, 7(11): 15729–15747. doi: 10.3390/rs71115729

Petropoulos G, Carlson T N, Wooster M J et al., 2009. A review of Ts/VI remote sensing based methods for the retrieval of land surface energy fluxes and soil surface moisture. *Progress in Physical Geography:Earth and Environment*, 33(2): 224–250. doi: 10.1177/0309133309338997

Prihodko L, Goward S N, 1997. Estimation of air temperature from remotely sensed surface observations. *Remote Sensing of Environment*, 60(3): 335–346. doi: 10.1016/S0034-4257(96)00216-7

Price J C, 1990. Using spatial context in satellite data to infer regional scale evapotranspiration. *IEEE Transactions on Geoscience & Remote Sensing*, 28(5): 940–948. doi: 10.1109/36.58983

Prince S D, Goetz S J, Dubayah R O et al. , 1998. Inference of surface and air temperature, atmospheric precipitable water and vapor pressure deficit using Advanced Very High-Resolution Radiometer satellite observations: comparison with field observations. *Journal of Hydrology*, 212–213: 230−249. doi: 10.1016/S0022-1694(98)00210-8

Qiu L J, Wu Y P, Shi Z Y et al., 2021. Quantifying spatiotemporal variations in soil moisture driven by vegetation restoration on the Loess Plateau of China. *Journal of Hydrology*, 600: 126580. doi: 10.1016/j.jhydrol.2021.126580

Rahimzadeh-Bajgiran P, Berg A A, Champagne C et al., 2013. Estimation of soil moisture using optical/thermal infrared remote sensing in the Canadian Prairies. *ISPRS Journal of Photogrammetry and Remote Sensing*, 83: 94–103. doi: 10.1016/j.isprsjprs.2013.06.004

Rahimzadeh-Bajgiran P, Omasa K, Shimizu Y, 2012. Comparative evaluation of the Vegetation Dryness Index (VDI), the Temperature Vegetation Dryness Index (TVDI) and the improved TVDI (iTVDI) for water stress detection in semi-arid regions of Iran. *ISPRS Journal of Photogrammetry and Remote Sensing*, 68: 1–12. doi: 10.1016/j.isprsjprs.2011.10.009

Ren L S, Zhang S R, Guo X L et al., 2021. Interannual variation in riparian vegetation cover and its relationship with river flow under a high level of human intervention: an example from the Yongding River Basin. *Environmental Monitoring and Assessment*, 193(7): 406. doi: 10.1007/s10661-021-09187-8

Sadeghi M, Babaeian E, Tuller M et al., 2017. The optical trapezoid model: a novel approach to remote sensing of soil moisture applied to Sentinel-2 and Landsat-8 observations. *Remote Sensing of Environment*, 198: 52–68. doi: 10.1016/j.rse.2017.05.041

Sandholt I, Rasmussen K, Andersen J, 2002. A simple interpretation of the surface temperature/vegetation index space for assessment of surface moisture status. *Remote Sensing of Environment*, 79(2-3): 213–224. doi: 10.1016/S0034-4257(01)00274-7

Shifaw E, Sha J M, Li X M et al., 2018. Spatiotemporal analysis of vegetation cover (1984–2017) and modelling of its change drivers, the case of Pingtan Island, China. *Modeling Earth Systems and Environment*, 4(3): 899–917. doi: 10.1007/s40808-018-0473-6

Son N T, Chen C F, Chen C R et al., 2012. Monitoring agricultural drought in the Lower Mekong Basin using MODIS NDVI and land surface temperature data. *International Journal of Applied Earth Observation and Geoinformation*, 18: 417–427. doi: 10.1016/j.jag.2012.03.014

Stisen S, Sandholt I, Nørgaard A et al., 2008. Combining the triangle method with thermal inertia to estimate regional evapotranspiration: applied to MSG-SEVIRI data in the Senegal River basin. *Remote Sensing of Environment*, 112(3): 1242–1255. doi: 10.1016/j.rse.2007.08.013

Sun F X, Lü Y H, Fu B J et al., 2014. Spatial explicit soil moisture analysis: pattern and its stability at small catchment scale in the loess hilly region of china. *Hydrological Processes*, 28(13): 4091–4109. doi: 10.1002/hyp.9940

Sun L, Sun R, Li X W et al. , 2012. Monitoring surface soil moisture status based on remotely sensed surface temperature and vegetation index information. *Agricultural and Forest Meteorology*, 166 –167: 175 –187. doi: 10.1016/j.agrformet.2012.07.015

Tang R L, Li Z L, Tang B H, 2010. An application of the Ts-VI triangle method with enhanced edges determination for evapotranspiration estimation from MODIS data in arid and semi-arid regions: implementation and validation. *Remote Sensing of Environment*, 114(3): 540–551. doi: 10.1016/j.rse.2009.10.012

Wang J, Ling Z W, Wang Y et al., 2016. Improving spatial representation of soil moisture by integration of microwave observations and the temperature-vegetation-drought index derived from MODIS products. *Isprs Journal of Photogrammetry & Remote Sensing*, 113: 144–154. doi: 10.1016/j.isprsjprs.2016.01.009

Wang Lixia, Ren Zhiyuan, 2006. Quantificational analysis on eco-

water requirement of plant-soil compound ecosystem based on GIS: a case study of Yan'an Region in Northwest China. *Acta Geographica Sinica*, 61(7): 763–770. (in Chinese)

Wang Y F, Cao S X, 2011. Carbon sequestration may have negative impacts on ecosystem health. *Environmental Science & Technology*, 45(5): 1759–1760. doi: 10.1021/es200042s

Yu B W, Liu G H, Liu Q S, 2020. Effects of land use changes for ecological restoration on soil moisture on the Chinese Loess Plateau: a meta-analytical approach. *Journal of Forestry Research*, 31(2): 443–452. doi: 10.1007/s11676-018-0760-0

Zhang R H, Tian J, Su H B et al., 2008. Two improvements of an operational two-layer model for terrestrial surface heat flux retrieval. *Sensors*, 8(10): 6165–6187. doi: 10.3390/s8106165

Zhang X L, Zhang G D, Hu C H et al., 2020. Response of soil moisture to landscape restoration in the hilly and gully region of the Loess Plateau, China. *Biologia*, 75(6): 827–839. doi: 10.2478/s11756-020-00520-z

Zhu W B, Lv A F, Jia S F et al., 2017a. Development and evaluation of the MTVDI for soil moisture monitoring. *Journal of Geophysical Research:Atmospheres*, 122(11): 5533–5555. doi: 10.1002/2017JD026607

Zhu W B, Lü A F, Jia S F et al., 2017b. Retrievals of all-weather daytime air temperature from MODIS products. *Remote Sensing of Environment*, 189: 152–163. doi: 10.1016/j.rse.2016.11.011

Zhu W B, Jia S F, Lv A F, 2017c. A time domain solution of the Modified Temperature Vegetation Dryness Index (MTVDI) for continuous soil moisture monitoring. *Remote Sensing of Environment*, 200: 1–17. doi: 10.1016/j.rse.2017.07.032